PHYSICAL REVIEW C **66**, 012801(R) (2002)

Microscopic study of slablike and rodlike nuclei: Quantum molecular dynamics approach

Gentaro Watanabe,[1,2] Katsuhiko Sato,[1,3] Kenji Yasuoka,[4] and Toshikazu Ebisuzaki[2]
[1]*Department of Physics, University of Tokyo, Tokyo 113-0033, Japan*
[2]*Division of Computational Science, RIKEN, Saitama 351-0198, Japan*
[3]*Research Center for the Early Universe, University of Tokyo, Tokyo 113-0033, Japan*
[4]*Department of Mechanical Engineering, Keio University, Yokohama 223-8522, Japan*
(Received 13 May 2002; published 30 July 2002)

The structure of cold dense matter at subnuclear densities is investigated by quantum molecular dynamics simulations. We succeeded in showing that the phases with slablike and rodlike nuclei, etc., can be formed dynamically from hot uniform nuclear matter without any assumptions on nuclear shape. We also observe intermediate phases, which have complicated nuclear shapes. Geometrical structures of matter are analyzed with Minkowski functionals, and it is found that intermediate phases can be characterized as those with negative Euler characteristic. Our result suggests the existence of these kinds of phases in addition to the simple ''pasta'' phases in neutron star crusts.

DOI: 10.1103/PhysRevC.66.012801 PACS number(s): 21.65.+f, 26.50.+x, 26.60.+c, 02.70.Ns

Collapse-driven supernovas (SNs) and the subsequent formation of neutron stars (NSs) are the most dramatic processes during stellar evolution. These objects provide not only astrophysically significant phenomena but also interesting material phases inside them; both are strongly connected with each other. Investigating the properties of nuclear matter under extreme conditions is one of the essential topics for clarifying the mechanism of collapse-driven SNs [1] and the structure of NS crusts [2]. This subject is also interesting in terms of the fundamental problem of the complex fluids of nucleons.

At subnuclear densities, where nuclei are about to melt into uniform matter, it is expected that the energetically favorable configuration possesses interesting spatial structures such as rodlike and slablike nuclei and rodlike and spherical bubbles, etc., which are called nuclear ''pasta.'' This picture was first proposed by Ravenhall *et al.* [3] and Hashimoto *et al.* [4]. These works, which are based on free energy calculations with liquid drop models assuming some specific nuclear shapes, clarify that the most energetically stable nuclear shape is determined by a subtle balance between the nuclear surface and Coulomb energies. Although detailed aspects of phase diagrams vary with nuclear models [5], the realization of the pasta phases as energy minimum states can be seen in a wide range of nuclear models and the basic feature of the phase diagrams is universal [6,7] i.e., with increasing density, the shape of the nuclear matter region changes as sphere → cylinder → slab → cylindrical hole → spherical hole → uniform. This feature is also reproduced by Thomas-Fermi calculations [8–10]

The phases with these exotic nuclear structures, if they are realized in NS crusts or SN cores, bring about many astrophysical consequences. As for those in NS phenomena, it is interesting to note the relevance of the nonspherical nuclei in neutron star matter (NSM) to pulsar glitches [11] and the cooling of NSs [5]. For supernova matter (SNM), pasta phases are expected to affect the neutrino transport [3,7] and hydrodynamics in SN cores [9].

Though the properties of pasta phases in equilibrium state have been investigated actively, their formation and melting processes have not been discussed except for some limited cases based on perturbative approaches [2,12]. It is important to adopt a microscopic and dynamical approach, which allows arbitrary nuclear structures to understand these processes of nonspherical nuclei. At finite temperatures, it is considered that not only the nuclear surface becomes obscure but also the nuclei of various shapes may coexist. Therefore, it is necessary to incorporate density fluctuations without any assumptions on nuclear shape to investigate the properties of pasta phases at finite temperatures. Although some previous works [8,9] do not assume nuclear structure, they cannot incorporate fluctuations of nucleon distributions satisfactorily because they are based on the Thomas-Fermi calculation, which is a one-body approximation. In addition, only one structure is contained in the simulation box in these works; there are thus possibilities that nuclear shape is strongly affected by the boundary effect and some structures are prohibited implicitly.

We have started studying dense matter at subnuclear densities by quantum molecular dynamics (QMD) [13], which is one of the molecular dynamics (MD) approaches for nucleon many-body systems (see, e.g., Ref. [14] for review). MD for nucleons including QMD, which is a microscopic and dynamical method without any assumptions on nuclear structure, is suitable for incorporating fluctuations of particle distributions. The final aim of our study is to understand the above mentioned formation and melting processes of nonspherical nuclei and to investigate the properties of matter consisting of nonspherical nuclei at finite temperatures. For the first step, the question posed in this paper is as follows: *Can the phases with nonspherical nuclei be formed dynamically?*

There is a pioneering work by Maruyama *et al.* [15] which attempts to investigate the structure of matter at subnuclear densities by QMD. Unfortunately, they did not treat the Coulomb interaction consistently and could not anneal the system successfully. As a result, they could not reproduce the phases with nonspherical nuclei of simple structures. In the present work, we improve the above shortcomings and obtain phase diagrams for cold dense matter of proton frac-

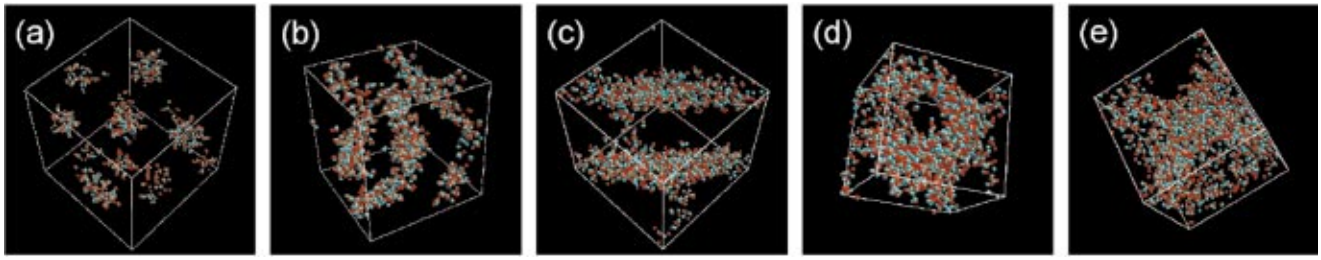

FIG. 1. (Color) The nucleon distributions of typical phases with simple structures of cold matter at $x=0.5$; (a) sphere phase, $0.1\rho_0$($D=43.65$ fm,$N=1372$); (b) cylinder phase, $0.18\rho_0$($D=41.01$ fm,$N=2048$); (c) slab phase, $0.4\rho_0$($D=31.42$ fm,$N=2048$); (d) cylindrical hole phase, $0.5\rho_0$($D=29.17$ fm, $N=2048$); and (e) spherical hole phase, $0.6\rho_0$($D=27.45$ fm,$N=2048$), where D is the box size. The red particles represent protons and the green ones represent neutrons.

tion $x=0.3$ and 0.5 at subnuclear densities. We also discuss nuclear shape changes with morphological measures.

While there are a lot of versions of MD for fermions, we choose QMD among them based on a trade-off between calculational amounts and accuracies. The typical length scale l of the interstructure is $l\sim 10$ fm and the density region of interest is just below the normal nuclear density $\rho_0 = 0.165$ fm^{-3}. The required nucleon number N in order to reproduce n structures in the simulation box is about $N \sim \rho_0(nl)^3$ (for slabs), it is thus desirable that we prepare nucleons of the order of 10 000 if we try to reduce boundary effects. While it is a very hard task to treat such a large system by, for example, fermionic molecular dynamics (FMD) and antisymmetrized molecular dynamics (AMD) (see, e.g., Ref. [14] and references therein) whose calculational amounts scale as $\sim N^4$, it is feasible to do it by QMD whose calculational amounts scale as $\sim N^2$. It is also noted that we mainly focus on macroscopic structures; the exchange effect would not be so important for them. Therefore, QMD, which is less elaborate in treating the exchange effect, has the advantages of the other models.

We have performed QMD simulations of an infinite (n,p,e) system with fixed proton fractions $x=0.3$ and 0.5 for various nucleon densities ρ [the density region is $(0.05–1.0)\rho_0$]. We set a cubic box, which is the imposed periodic boundary condition in which 2048 nucleons (1372 nucleons in some cases) are contained. The relativistic degenerate electrons which ensure the charge neutrality are treated as a uniform background and the Coulomb interaction is calculated by the Ewald method (see, e.g., Ref. [16]), which enables us to sum contributions of long-range interactions in a system with periodic boundary conditions. For nuclear interaction, we use an effective Hamiltonian developed by Maruyama *et al.* (medium equation of state model) [15], which reproduces the bulk properties of nuclear matter and the properties of stable nuclei, especially heavier ones, i.e., binding energy and root-mean-square radius.

We first prepare a uniform hot nucleon gas at $k_BT \sim 20$ MeV as an initial condition, which is equilibrated for $\sim 500–2000$ fm/c in advance. In order to realize the ground state of matter, we then cool it down slowly for $O(10^3–10^4)$ fm/c keeping the nucleon density constant by the frictional relaxation method, etc. until the temperature becomes ~ 0.1 MeV or less. Note that any artificial fluctuations are not given during the simulation.

The QMD equations of motion with friction terms are solved using the fourth-order Gear predictor-corrector method in conjunction with the multiple time step algorithm [16]. Integration time steps Δt are set to be adaptive in the range of $\Delta t<0.1–0.2$ fm/c depending on the degree of convergence. At each step, the correcting operation is iterated until the error of position Δr and the relative error of momentum $\Delta p/p$ become smaller than 10^{-6}, where Δr and $\Delta p/p$ are estimated as the maximum values of correction among all particles. Computer systems which we use are equipped with MD-GRAPEII.

Shown in Figs. 1 and 2 are the resultant nucleon distributions of cold matter at $x=0.5$ and 0.3, respectively. We can see from these figures that the phases with rodlike and slablike nuclei, cylindrical and spherical bubbles, in addition to those one with spherical nuclei, are reproduced in both the cases. We would like to mention here some reasons of discrepancies between the present result and the result obtained by Maruyama *et al.*, which says that *the nuclear shape may not have these simple symmetries* [15]. The most crucial rea-

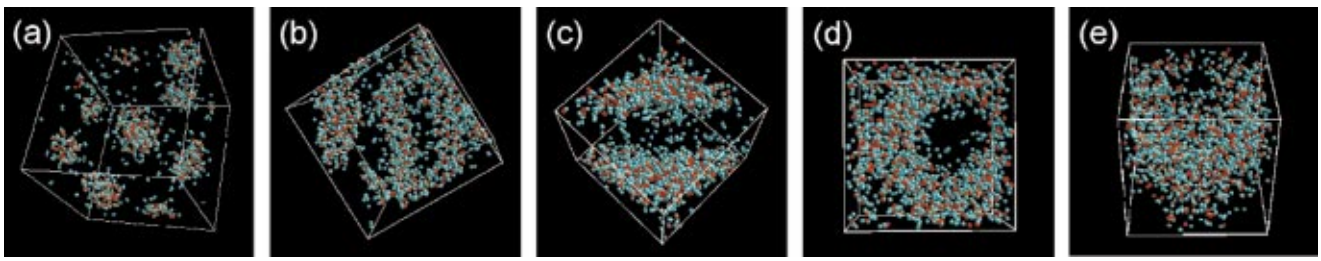

FIG. 2. (Color) Same as Fig. 1 at $x=0.3$; (a) sphere phase, $0.1\rho_0$($D=49.88$ fm,$N=2048$); (b) cylinder phase, $0.18\rho_0$($D=41.01$ fm,$N=2048$); (c) slab phase, $0.35\rho_0$($D=32.85$ fm,$N=2048$); (d) cylindrical hole phase, $0.5\rho_0$($D=29.17$ fm,$N=2048$); and (e) spherical hole phase, $0.55\rho_0$($D=28.26$ fm,$N=2048$). The red particles represent protons and the green ones represent neutrons.

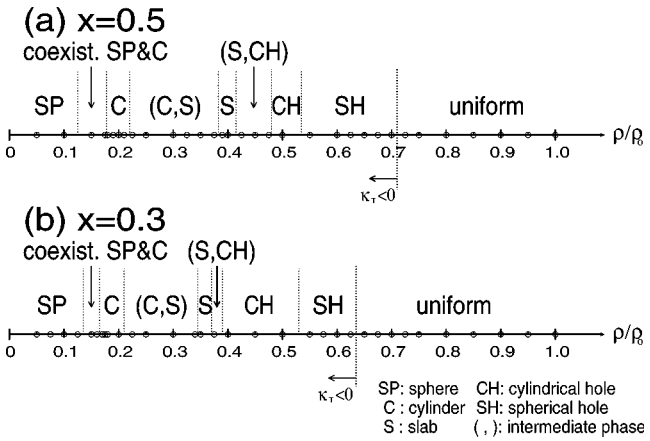

FIG. 3. Phase diagrams of cold matter at $x=0.5$ (a) and $x=0.3$ (b). Matter is unstable against phase separation in the density region shown as $\kappa_T<0$, where κ_T is the isothermal compressibility. The symbols SP, C, S, CH, and SH stand for nuclear shapes, i.e., sphere, cylinder, slab, cylindrical hole and spherical hole, respectively. The (A,B) show intermediate phases between the A phase and B phase suggested in this work. They have complicated structures different from those of both the A phase and Bphase. Simulations have been carried out at densities denoted by small circles.

son seems to be the difference in the treatment of the Coulomb interaction. In the present simulation, we calculate the long-range Coulomb interaction in a consistent way using the Ewald method. For the system of interest where the Thomas-Fermi screening length is comparable to or larger than the size of nuclei, this treatment is more adequate than that with introducing an artificial cutoff distance as in Ref. [15]. The second reason would be the difference in the relaxation time scales τ. In our simulation, we can reproduce the bubble phases [see (d) and (e) of Figs. 1 and 2] with $\tau \sim 10^3$ fm/c and the nucleus phases [see (b) and (c) of Figs. 1 and 2] with $\tau \sim O(10^4)$ fm/c. However, the matter in the density region corresponding to a nucleus phase is quenched in an amorphous state when $\tau \lesssim 10^3$ fm/c. In the present work, we take τ much larger than the typical time scale $\tau_{th} \sim O(100)$ fm/c for nucleons to thermally diffuse in the distance of $l \sim 10$ fm at $\rho \simeq \rho_0$ and $k_B T \simeq 1$ MeV. This temperature is below the typical value of the liquid-gas phase transition temperature in the density region of interest, it is thus considered that our results are thermally relaxed in a satisfying level.

Phase diagrams of matter in the ground state are shown in Figs. 3(a) and 3(b) for $x=0.5$ and 0.3, respectively. As can be seen from these figures, the obtained phase diagrams basically reproduce the sequence of the energetically favored nuclear shapes predicted by simple discussions [4], which only take account of the Coulomb and surface effects; this prediction is that the nuclear shape changes as sphere → cylinder → slab → cylindrical hole → spherical hole → uniform, with increasing density. Comparing Figs. 3(a) and 3(b), we can see that the phase diagram shifts towards the lower density side with decreasing x, which is due to the tendency that as the nuclear matter becomes more neutron-rich, the saturation density is lowered. It is remarkable that the density dependence of the nuclear shape, except for cylindrical bubbles (just in the case of $x=0.3$) and spherical nuclei and bubbles, is quite sensitive and phases with intermediate nuclear shapes, which are not simple as shown in Figs. 1 and 2, are observed in two density regions: one is between the cylinder phase and the slab phase, the other is between the slab phase and the cylindrical hole phase. We note that these phases are different from coexistence phases with nuclei of simple shapes and we will refer to them as intermediate phases.

To extract the morphological characteristics of the nuclear shape changes and the intermediate phases, we introduce the Minkowski functionals (see, e.g., Ref. [17] and references therein) as geometrical and topological measures of the nuclear surface. Let us consider a homogeneous body $K \in \mathcal{R}$ in the d-dimensional Euclidean space, where $\mathcal{R}$ is the class of such bodies. Morphological measures are defined as functionals $\varphi: \mathcal{R} \to \mathbf{R}$ which satisfy the following three properties: (1) *Motion invariance*, i.e., $\varphi(K)=\varphi(gK)$, where g denotes any translations and rotations; (2) *Additivity*, i.e., $\varphi(K_1 \cup K_2)=\varphi(K_1)+\varphi(K_2)-\varphi(K_1 \cap K_2)$, where $K_1, K_2 \in \mathcal{R}$; (3) *Continuity*, i.e., $\lim_{n\to\infty}\varphi(K_n)=\varphi(K)$ if $\lim_{n\to\infty}K_n=K$, where K is a convex body and $\{K_n\}$ is a sequence of convex bodies. Hadwiger's theorem states that there are just $d+1$ independent functionals which satisfy the above properties; they are known as Minkowski functionals. In three-dimensional space, four Minkowski functionals are related to the volume, the surface area, the integral mean curvature, and the Euler characteristic.

Here, we particularly focus on the integral mean curvature and the Euler characteristic; the results of other quantities will be discussed elsewhere. Both are described by surface integrals of the following local quantities, the mean curvature $H=(\kappa_1+\kappa_2)/2$ and the Gaussian curvature $G=\kappa_1\kappa_2$, i.e., $\int_{\partial K} H dA$ and $\chi \equiv (1/2\pi)\int_{\partial K} G dA$, where κ_1 and κ_2 are the principal curvatures and dA is the area element of the surface of the body K. The Euler characteristic χ is a purely topological quantity and

$$\chi = (\text{number of isolated regions}) - (\text{number of tunnels}) + (\text{number of cavities}). \quad (1)$$

Thus $\chi>0$ for the sphere and the spherical hole phases and the coexistence phase of spheres and cylinders, and $\chi=0$ for the other ideal pasta phases, i.e., the cylinder, the slab, and the cylindrical hole phases. We introduce the area-averaged mean curvature $\langle H \rangle \equiv (1/A)\int H dA$ and the Euler characteristic density χ/V as normalized quantities, where V is the volume of the whole space.

We calculate these quantities by the following procedure. We first construct proton and nucleon density distributions, $\rho_p(\mathbf{r})=|\Phi_p(\mathbf{r})|^2$ and $\rho(\mathbf{r})=|\Phi(\mathbf{r})|^2$, from the data of the centers of position of the nucleons, where $\Phi_p(\mathbf{r})$ and $\Phi(\mathbf{r})$ are the QMD trial wave functions of protons and nucleons (see Ref. [15]). We set a threshold proton density $\rho_{p,th}$ and then calculate $f(\rho_{p,th}) \equiv V(\rho_{p,th})/A(\rho_{p,th})$, where $V(\rho_{p,th})$ and $A(\rho_{p,th})$ are the volume and the surface areas of the regions in which $\rho_p(\mathbf{r}) \geqslant \rho_{p,th}$. We find out the value $\rho_{p,th}$

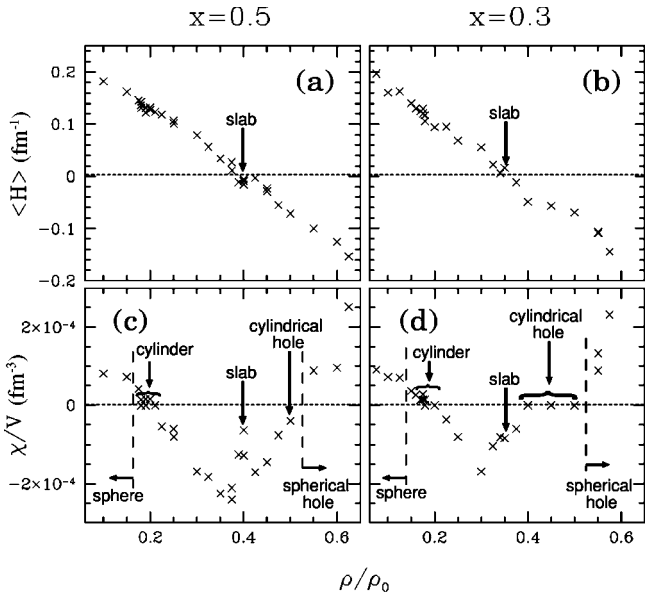

FIG. 4. Density dependence of the Minkowski functionals of cold matter at $x=0.5$ [(a) and (c)] and $x=0.3$ [(b) and (d)].

$=\rho^*_{\mathrm{p,th}}$, where $(d^2/d\rho^2_{\mathrm{p,th}})f(\rho^*_{\mathrm{p,th}})=0$, and define the regions in which $\rho_{\mathrm{p}}(\mathbf{r})\geqslant\rho^*_{\mathrm{p,th}}$ as nuclear regions. For spherical nuclei, for example, $\rho^*_{\mathrm{p,th}}$ corresponds to a point of inflection of a radial density distribution. In almost the whole phase-separating region, the values of ρ^*_{th} are distributed in the range of about $(0.7–0.9)\rho_0$ in both the cases of $x=0.5$ and 0.3, where ρ^*_{th} is the threshold nucleon density corresponding to $\rho^*_{\mathrm{p,th}}$. We then calculate A, $\int HdA$, and χ for the determined nuclear surface. We evaluate A by the triangle decomposition method, $\int HdA$ by the algorithm shown in Ref. [17] in conjunction with a calibration by correction of surface area, and χ by the algorithm of Ref. [17] and by that of counting deficit angles [18], which confirms that both of them give the same results.

We have plotted the obtained ρ dependence of $\langle H\rangle$ and χ/V for the surface of $\rho_{th}=\rho^*_{th}$ in Fig. 4. In addition to the values of $\langle H\rangle$ for the surface of $\rho_{th}=\rho^*_{th}$, we have also investigated those for the surface of $\rho_{th}=\rho^*_{th}\pm0.05\rho_0$ to examine the extent of the uncertainties of this quantity, which stem from the arbitrariness in the definition of the nuclear surface, but we could not observe remarkable differences from the values for $\rho_{th}=\rho^*_{th}$ (they were smaller than 0.015/fm). We could not see these kinds of uncertainties in χ/V, except for the densities near below the density at which matter turns uniform.

The behavior of $\langle H\rangle$ shows that it decreases almost monotonical from positive to negative with increasing ρ until the matter turns uniform. The densities corresponding to $\langle H\rangle\simeq0$ are about $0.4\rho_0$ and $0.35\rho_0$ for $x=0.5$ and 0.3, respectively; these values are consistent with the density regions of the phase with slablike nuclei (see Fig. 3). As mentioned previously, χ/V is actually positive in the density regions corresponding to the phases with spherical nuclei, coexistence of spherical and cylindrical nuclei, and spherical holes because of the existence of isolated regions. As for those corresponding to the phases with cylindrical nuclei, planar nuclei, and cylindrical holes, $\chi/V\simeq0$. The fact that the values of χ/V are not exactly zero for nucleon distributions shown as slab phases in Figs. 1 and 2 reflects the imperfection of these slabs, which is due to the small nuclear parts which connect the neighboring slabs. However, we can say that the behavior of χ/V depicted in Figs. 4(c) and 4(d) shows that χ/V is negative in the density regions of the intermediate phases, even if we take account of the imperfection of the obtained nuclear shapes and the uncertainties of the definition of the nuclear surface. This means that the intermediate phases consist of nuclear surfaces, which are saddlelike at each point on average, and each of them consists of highly connected nuclear and gas regions due to a lot of tunnels [see Eq. (1)].

Let us now refer to discrepancies from the results of previous works which do not assume nuclear structure [8,9]; the intermediate phases cannot be seen in these works. We can give the following two reasons for the discrepancies.

(1) These previous calculations are based on the Thomas-Fermi approximation which cannot sufficiently incorporate fluctuations of nucleon distributions. This shortcoming may result in favoring nuclei of smoothed simple shapes than in the real situation.

(2) There is a large possibility that some highly connected structures which have two or more substructures in a period are neglected in these works because only one structure is contained in a simulation box.

If the phases with highly connected nuclear and bubble regions are realized as the most energetically stable states, we can say that it is not an unnatural thing [19]. It is considered that, for example, a phase with perforated slablike nuclei, which has negative χ/V, could be more energetically stable than that with extremely thin slablike nuclei. The thin planar nucleus costs surface-surface energy, which stems from the fact that nucleons in it feel the surfaces of both sides. We have to examine the existence of the intermediate phases by more extensive simulations with larger nucleon numbers and with longer relaxation time scales in the future.

Here we would like to discuss the astrophysical consequences of our results. Pethick and Potekhin have pointed out that pasta phases with rodlike and slablike nuclei are analogous to the liquid crystals according to the similarity of the geometrical structures [11]. It can also be said that the intermediate phases observed in the present work are ''spongelike'' phases because they have both highly connected nuclear and bubble regions shown as $\chi/V<0$. The elastic properties of the spongelike intermediate phases are qualitatively different from those of the liquid-crystal-like pasta phases because the former ones do not have any directions in which the restoring force does not act; on the other hand the latter ones have. Our results suggest that the intermediate phases occupy a significant fraction of the density region in which nonspherical nuclei can be seen (see Fig. 3). If this is also true for the more neutron-rich case as $x\sim0.1$, it leads to the increase of the maximum elastic energy that can be stored in the NS crust, higher than that in the case where all nonspherical nuclei have simple structures. Besides, the cylinder and the slab phases, which are liquid-crystal-like, lie

between the spongelike intermediate phases or the crystalline solidlike phase, and the releasing of the strain energy would, in consequence, concentrate on the domain of these liquid-crystal-like phases. The above mentioned effects of the intermediate phases should be taken into account in considering the crust dynamics of starquakes, etc. if these phases exist in NSM. In the context of pulsar glitch phenomena, the effects of the spongelike nuclei on the pinning rate of superfluid neutron vortices also have yet to be investigated.

For neutrino cooling of NSs, some version of the direct URCA process which is suggested by Lorenz *et al.* [5], that this might be allowed in the pasta phases, would be suppressed in the intermediate phases. This is due to the fact that the proton spectrum is no longer continuous in the spongelike nuclei. The last point which we would like to mention is about the effects of the intermediate phases on neutrino trapping in SN cores. The nuclear parts connect over a wide region, which is much larger than that characterized by the typical neutrino wavelength ~ 20 fm. Thus the neutrino scattering processes are no longer coherent in contrast to the case of the spherical nuclei, and this may, in consequence, reduce the diffusion time scale of neutrinos as in the case of pasta phases with simple structures. This reduction softens the SNM and would thus act to enhance the amount of the released gravitational energy.

Our calculations demonstrate that the pasta phases can be formed dynamically from hot uniform matter in the proton-rich cases of $x=0.5$ and 0.3 without any assumptions on nuclear shape. This suggests the existence of these phases in NS crusts because they cool down keeping the local thermal equilibrium after proto-NSs are formed and their cooling time scale is much larger than the relaxation time scale of our simulations. This conclusion has to be confirmed in more neutron-rich cases of $x\sim 0.1$ in the future. Our results also suggest the existence of the highly connected intermediate phases which are characterized as $\chi/V<0$. This provides a vivid picture that NS inner crusts which consist of dense matter at subnuclear densities may be rich in properties due to the possibilities of a variety of material phases.

G.W. is grateful to T. Maruyama, K. Iida, K. Niita, A. Tohsaki, K. Oyamatsu, S. Chikazumi, C. Hikage, and K. Kotake for helpful discussions and comments. This work was supported in part by the Junior Research Associate Program in RIKEN through Research Grant No. J130026 and by Grants-in-Aid for Scientific Research provided by the Ministry of Education, Culture, Sports, Science and Technology through Research Grants No. 14102004 and 14-7939.

[1] H.A. Bethe, Rev. Mod. Phys. **62**, 801 (1990).
[2] C.J. Pethick and D.G. Ravenhall, Annu. Rev. Nucl. Part. Sci. **45**, 429 (1995).
[3] D.G. Ravenhall, C.J. Pethick, and J.R. Wilson, Phys. Rev. Lett. **50**, 2066 (1983).
[4] M. Hashimoto, H. Seki, and M. Yamada, Prog. Theor. Phys. **71**, 320 (1984).
[5] C.P. Lorenz, D.G. Ravenhall, and C.J. Pethick, Phys. Rev. Lett. **70**, 379 (1993).
[6] G. Watanabe, K. Iida, and K. Sato, Nucl. Phys. **A676**, 455 (2000).
[7] G. Watanabe, K. Iida, and K. Sato, Nucl. Phys. **A687**, 512 (2001).
[8] R.D. Williams and S.E. Koonin, Nucl. Phys. **A435**, 844 (1985).
[9] M. Lassaut *et al.*, Astron. Astrophys. **183**, L3 (1987).
[10] K. Oyamatsu, Nucl. Phys. **A561**, 431 (1993).
[11] C.J. Pethick and A.Y. Potekhin, Phys. Lett. B **427**, 7 (1998).
[12] K. Iida, G. Watanabe, and K. Sato, Prog. Theor. Phys. **106**, 551 (2001).
[13] J. Aichelin and H. Stöcker, Phys. Lett. B **176**, 14 (1986).
[14] H. Feldmeier and J. Schnack, Rev. Mod. Phys. **72**, 655 (2000).
[15] T. Maruyama *et al.*, Phys. Rev. C **57**, 655 (1998).
[16] M.P. Allen and D.J. Tildesley, *Computer Simulation of Liquids* (Clarendon, Oxford, 1987).
[17] K. Michielsen and H. De Raedt, Phys. Rep. **347**, 461 (2001).
[18] J.R. Gott III, A.L. Melott, and M. Dickinson, Astrophys. J. **306**, 341 (1986); D.H. Weinberg, Publ. Astron. Soc. Pac. **100**, 1373 (1988).
[19] Existence of some phase with a complicated structure is also suggested by P. Magierski, and P.H. Heenen, Phys. Rev. C **65**, 045804 (2002). They focus on shell effects of dripped neutrons.